Micellization of ω-Functionalized Diblock Copolymers in Selective Solvent. Study on the Effect of Hydrogen Bonds

A. Karatzas, M. Talelli, T. Vasilakopoulos, M. Pitsikalis,* and N. Hadjichristidis*

Department of Chemistry, University of Athens, Panepistimiopolis Zographou 15771 Athens Greece

Received June 22, 2006; Revised Manuscript Received August 23, 2006

ABSTRACT: Two series of ω-functionalized diblock copolymers polystyrene-*b*-polyisoprene, PS−PI, having hydroxyl end groups either at the PS (PI−PS−OH) or at the PI (PS−PI−OH) block were synthesized by living anionic polymerization. The samples had similar molecular weights but different compositions. Employing suitable post-polymerization reactions the hydroxyl groups were transformed to the corresponding 2-ureido-4-pyrimidinone (UPy) functions. The UPy group is known to dimerize strongly in a self-complementary array of four cooperative hydrogen bonds. The micellization properties of the unfunctionalized and the ω-functionalized polymers having either hydroxyl or UPy end groups were studied in *n*-decane, which is a selective solvent for the PI block, by static and dynamic light scattering and dilute solution viscometry. A distinct micellar behavior was obtained depending on the nature of the end group and their location either at the core-forming or the corona-forming block. To confirm the results regarding the effect of the hydrogen bonds the solid-state properties of the copolymers were studied by differential scanning calorimetry and thermogravimetric analysis. Furthermore, the dilute solution properties were investigated in chloroform, which is a common good solvent for both the PS and PI blocks but nonpolar, thus allowing the formation of hydrogen bonds.

Introduction

The field of supramolecular chemistry is well established. Intermolecular noncovalent interactions constitute the base of biology and biochemistry. Vital operations, like molecular transportation, conformation of proteins, and the evolution of genetic information are due to noncovalent bonds. Recently, there has been an effort to employ the features of supramolecular chemistry in nonbiological systems.[1−7] Noncovalent bonds, especially multiple hydrogen bonding,[8−27] and metal−ligand complexes[28−36] in molecular design have received significant attention, due to the ability of forming new supramolecular structures that exhibit thermoreversible characteristics. Dynamic systems[37−39] can be obtained through these noncovalent interactions. The association constants of these groups depend on the temperature, the solvent and the solution concentration.

Meijer et al.[40−42] introduced 2-ureido-4-pyrimidone (UPy) as a structural unit for the formation of supramolecular polymers. This group can dimerize via a strong quadruple hydrogen bond array in common organic solvents. With an association constant of $K_{assoc} = 6 \times 10^7$ M^{-1} in chloroform and a facile and quantitative synthesis through a one step procedure, it is an appropriate compound for the preparation of supramolecular structures via molecular recognition.

New horizons are emerged in materials science through the combination of supramolecular and polymer chemistry. The incorporation to a polymeric chain of functional groups, which form noncovalent bonds, leads to a material with novel properties. Recently, Long et al.[43−47] have studied several functionalized macromolecules. UPy and other functional groups have been attached to polystyrene, PS, polyisoprene, PI, and polystyrene-*b*-polyisoprene, PS-*b*-PI, as well as to other polymeric chains. Rheological and thermal studies led to the conclusion that due to hydrogen bonds reversible aggregates are formed in bulk. These aggregates are stable up to 80 °C. Viscometry studies, conducted on polyacrylates containing 10 mol % UPy groups, revealed that strong aggregates were formed only in nonpolar solvents such as toluene and chloroform. In polar solvents, supramolecular structures were not produced. The size and the stability of these aggregates depend on the number of UPy units at each macromolecular chain and the solution concentration.

In this study, we report the synthesis of well-defined ω-functionalized polystyrene-*b*-polyisoprene, PS−PI, diblock copolymers having hydroxyl- or 2-ureido-4-pyrimidinone, UPy, end groups either at the PS or the PI block with similar molecular weights and various compositions. Block copolymers are very useful polymeric materials.[48] One of their characteristics is the formation of micelles in selective solvents.[49−58] Above a concentration value, called the critical micelle concentration (cmc), diluted block copolymers in a selective solvent are organized in micelles. This phenomenon is reversible, and it depends on the temperature and the concentration of the solution. In most cases, block copolymer micelles are spherical with a compact core consisting of the insoluble blocks and a corona composed from the soluble ones.

The micellization behavior of the above-mentioned unfunctionalized and functionalized copolymers were studied in *n*-decane in order to trace the effect of hydrogen bonds on this procedure. The combination of two reversible phenomena, micellization of block copolymers and interactions through the formation of hydrogen bonds in a nonpolar solvent, leads to the development of a dynamic system which is responsive to its chemical environment and the temperature. The dilute solution properties of certain UPy-functionalized copolymers were also investigated in chloroform, which is a common good solvent for both the PS and PI blocks but nonpolar, thus allowing the formation of hydrogen bonds.

Experimental Section

Materials. The ω-functionalized diblock copolymers were prepared by anionic polymerization procedures under high-vacuum in all-glass reactors. Benzene was the polymerization solvent. The

* Corresponding authors. E-mail: (N.H.) hadjichristidis@chem.uoa.gr; (M.P.) pitsikalis@chem.uoa.gr.

10.1021/ma061396n CCC: $33.50
Published on Web 11/04/2006

Scheme 1. Reaction Scheme for the Synthesis of Unfunctionalized and Functionalized Diblock Copolymers

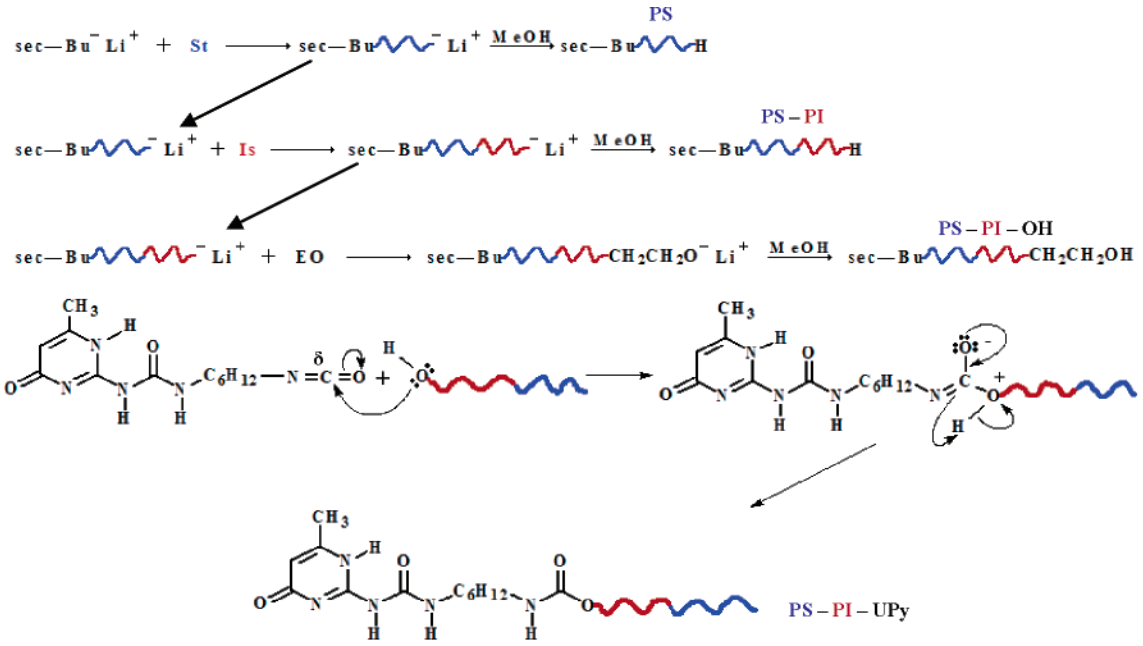

purification of the solvent and the monomers, styrene (S), isoprene (I), and ethylene oxide (EO) was performed according to well-known procedures.[59] *sec*-BuLi was prepared under vacuum by the reaction of *sec*-BuCl with a 6-fold excess of Li metal in hexane and was used as initiator. Degassed methanol was used to terminate the living polymers. The preparation of the UPy group and its incorporation to the polymeric chain was conducted according to published procedures.[40−42] $CHCl_3$ was dried over molecular sieves and distilled prior its use. All the other compounds and the solvent *n*-decane (Fluka, ≥95%) were used without any further purification.

Polymer Synthesis. As an example the synthesis of sample SIOH 46/54 is described. The polymerization reaction was performed in benzene (200 mL) at room temperature. Styrene (10.3 g) was polymerized first using *sec*-BuLi (2.06×10^{-3} mol) as initiator. A quantity of the living PSLi solution (40 mL, 2 g of polymer) was sampled for characterization. Isoprene (8.3 g) was then added, followed by the addition of an excess of ethylene oxide (10^{-2} mol). Under these conditions only one monomeric unit of ethylene oxide reacts with the living polymer chain.[60] Finally, the living polymer was terminated with degassed methanol. This procedure leads to the synthesis of PS−PI−OH diblock copolymers. Before the addition of ethylene oxide a sample of the living block copolymer was isolated and terminated with degassed methanol. This leads to the synthesis of two identical block copolymers, the unfunctionalized precursor and the corresponding functionalized one.

The synthesis of PI−PS−OH diblock copolymers involves initially the polymerization of isoprene followed by the addition of a small amount of tetrahydrofuran, THF, prior the addition of styrene in order to accelerate the cross-propagation reaction. The living PI−PSLi chains, thus produced, were reacted with ethylene oxide and then terminated with degassed methanol to afford the desired structures.

All the samples were precipitated in methanol. The final products were dried in a vacuum oven until constant weight. A typical reaction scheme is given in Scheme 1.

Functionalization Reaction for the Incorporation of the UPy Group. The hydroxyl-functionalized copolymers were transformed to the corresponding UPy-terminated samples using literature procedures.[21,42] A typical procedure involved the synthesis of UPy by reacting 0.70 mol of 2-amino-4-hydroxy-6-methylpyridine with 4.75 mol of 1,6-hexanediisocyanate and refluxing at 100 °C for 16 h. The UPy group was isolated by precipitation in *n*-pentane. The solid was dried at 50 °C under vacuum. 15 mmol of the copolymer were then dissolved in 500 mL of dried $CHCl_3$ followed by the addition of 70 mmol UPy and a few drops of the catalyst tin dilaureate. The reaction was allowed to proceed for 16 h at 60 °C under argon. The excess quantity of UPy is removed by successive dilutions-precipitations of the functionalized polymers. Toluene was used as solvent and methanol as nonsolvent.

Preparation of the Micellar Solutions. The block copolymers were dissolved in *n*-decane for the preparation of the stock solution. The samples were allowed to stand at room temperature for at least 24 h, then heated at 50 °C for 3 h to achieve equilibrium structures and finally left at room temperature for 24 h before the measurements. The stock solution was diluted to produce solutions of different concentrations. Stable micellar solutions were obtained without any polymer precipitation or visible change being noticed after standing at room temperature for several weeks.

Characterization Methods. SEC experiments were conducted at 40 °C using a modular instrument consisting of a Waters model 510 pump, a Waters model U6K sample injector, a Waters model 401 differential refractometer, a Waters model 486 UV spectrophotometer, and a set of four μ-Styragel columns with a continuous porosity range from 10^6 to 10^3 Å. The columns were housed in an oven thermostated at 40 °C. THF was the carrier solvent at a flow rate of 1 mL/min.

Multidetector SEC analysis [refractive index and two-angle laser light scattering detectors (SEC-TALLS)], using a Waters 1525 high-pressure liquid chromatography pump, Waters UltraStyragel columns (HR-2, HR-4, HR-5E, and HR-6E), a Waters 2410 differential refractometer detector, and a Precision 2020 two-angle (15°, 90°) light scattering detector were employed for the determination of the refractive index increments, d*n*/d*c* and the weight-average molecular weights of the samples.

Static light scattering measurements were performed with a Chromatix KMX-6 low angle laser light scattering photometer at 25 °C equipped with a 2 mW He−Ne laser operating at $\lambda = 633$ nm. The eq 1 describing the concentration dependence of the reduced intensity is

$$\frac{Kc}{\Delta R_\theta} = \frac{1}{M_w} + 2A_2c + \ldots \qquad (1)$$

where K is a combination of optical and physical constants, including the refractive index increment, dn/dc, and ΔR_θ, the excess Rayleigh ratio of the solution over that of the solvent. Stock solutions were prepared, followed by dilution with solvent to obtain appropriate concentrations. All solutions and solvents were optically

clarified by filtering through 0.22 μm pore size nylon filters directly into the scattering cell.

Refractive index increments, *dn*/d*c*, at 25 °C were also measured with a Chromatix KMX-16 refractometer operating at 633 nm and calibrated with aqueous NaCl solutions.

Dynamic light scattering measurements were conducted with a Series 4700 Malvern system composed of a PCS5101 goniometer with a PCS stepper motor controller, a Cyonics variable power Ar^+ laser, operating at 488 nm, a PCS8 temperature control unit, a RR98 pump/filtering unit and a 192 channel correlator for the accumulation of the data. The correlation functions were analyzed by the cumulant method and the CONTIN software. Measurements were carried out at 45, 90, and 135°. The angular dependence of the ratio Γ/q^2, where Γ is the decay rate of the correlation function and q is the scattering vector, was not very important for most of the micellar solutions. In these cases apparent translational diffusion coefficients at zero concentration, $D_{0,app}$ were measured using the eq 2:

$$D_{app} = D_{0,app}(1 + k_D c) \quad (2)$$

where k_D is the coefficient of the concentration dependence of the diffusion coefficient. The functionalized copolymers, having the −OH or −Upy groups at the PI chain end, the corona forming block, showed angular dependence. In this case the diffusion coefficient was obtained from the slope of the Γ/q^2 vs q plot. Apparent hydrodynamic radii at infinite dilutions, R_h, were calculated by aid of the Stokes−Einstein eq 3

$$R_h = kT/6\pi\eta_s D_{0,app} \quad (3)$$

where k is the Boltzmann's constant, T the absolute temperature, and η_s the viscosity of the solvent.

Viscometric data were analyzed using the Huggins eq 4

$$\frac{\eta_{sp}}{c} = [\eta] + K_H[\eta]^2 c + ... \quad (4)$$

and the Kraemer eq 5

$$\frac{\ln \eta_r}{c} = [\eta] + K_K[\eta]^2 c + ... \quad (5)$$

where η_r, η_{sp}, and $[\eta]$ are the relative, specific, and intrinsic viscosities respectively, K_H and K_K the Huggins and Kraemer constants, respectively. All the measurements were carried out at 25 °C except two cases, where the measurements were conducted at 40 and 45 °C. Cannon-Ubbelohde dilution viscometers equipped with a Schott-Geräte AVS 410 automatic flow timer were used. Viscometric radii, R_v, were calculated from the eq 6

$$R_v = \left(\frac{3}{10\pi N_A}\right)^{1/3} ([\eta] M_{w,app})^{1/3} \quad (6)$$

where $M_{w,app}$ is the weight-average molecular weight determined by light scattering measurements.

The ^{1}H NMR spectra were recorded in *d*-chloroform at 25 °C with a Varian Unity Plus 300/54 NMR spectrometer.

DSC experiments were performed with a 2910 Modulated DSC model from TA Instruments. The samples were heated or cooled at a rate of 10 °C/min.

TGA experiments were conducted with a Q50 model from TA Instruments. The heating rate was adjusted at 10 °C/min.

Results and Discussion

The samples are symbolized as SI denoting the presence of polystyrene, PS, and polyisoprene, PI, blocks. The functional end groups are indicated as OH or UPy. The following numbers refer to the wt % composition in PS and PI, calculated by ^{1}H NMR measurements in *d*-chloroform. For example SIUPy 46/54 is a diblock copolymer with PS and PI blocks having a UPy end group at the PI chain end and a composition 46wt % in PS and 54wt % in PI. The molecular characteristics of the diblock copolymers are summarized in Table 1.

Table 1. Molecular Characteristics of the Unfunctionalized Diblock Copolymers in THF

sample	$\overline{M_w}^a \times 10^{-3}$	$A_2{}^a \times 10^3$ mL·mol·g^{-2}	d*n*/d*c*^{b} (mL·g^{-1})	wt % PS^c	$\overline{M_w}/\overline{M_n}^d$
SI 33/67	10.5	0.94_5	0.138	33	1.03
SI 46/54	12.0	1.41	0.143	46	1.03
SI 64/36	24.1	1.32	0.166	64	1.03
IS 30/70	11.7	1.63	0.155	70	1.04
IS 52/48	12.0	1.40	0.149	48	1.03
IS 68/32	10.8	1.54	0.138	32	1.03

[a] By low angle laser light scattering (LALLS) in THF at 25 °C. [b] By differential refractometry in THF at 25 °C. [c] By ^{1}H NMR in *d*-chloroform at 25 °C. [d] By size exclusion chromatography (SEC).

Table 2. LALLS Results for the Series of SI and IS Diblock Copolymers in *n*-Decane at 25 °C

sample	$\overline{M_w} \times 10^{-3}$	$A_2 \times 10^5$ mL·mol·g^{-2}	d*n*/d*c*^{b} (mL·g^{-1})	$N_w{}^a$	wt % PS
SI 33/67	105.7	−7.70	0.132	10	33
SIOH 33/67	97.0	−32.6		9	33
SIUPy 33/67	−	−		−	33
SI 46/54	189.7	−40.8	0.135	16	46
SIOH 46/54	191.3	−71.5		16	46
SIUPy 46/54	−	−		−	46
SI 64/36	1089.0	−3.25	0.148	45	64
SIOH 64/36	1142.4	−1.50		47	64
SIUPy 64/36	−	−		−	64
IS 68/32	141.5	−47.8	0.131	11	32
ISOH 68/32	136.7	−16.2		11	32
ISUPy 68/32	125.5	−25.7		10	32
IS 52/48	200.1	−6.34	0.141	17	48
ISOH 52/48	194.7	−47.0		16	48
ISUPy 52/48	185.8	−33.2		15	48
IS 30/70	468.2	−5.48	0.150	38	70
ISOH 30/70	474.4	−8.16		39	70
ISUPy 30/70	492.7	−15.0		40	70

[a] Weight-average degree of association. [b] By differential refractometry in *n*-Decane at 25 °C.

Well-defined polymers with narrow molecular weight distributions and high molecular and compositional homogeneity were obtained. All the samples had similar molecular weights except SI 64/36. The molecular characterization was performed to the unfunctionalized polymers to avoid the complexity caused by possible association effects promoted by the functional end groups. SEC measurements were performed in $CHCl_3$ and THF in the presence of 5% triethylamine for the functionalized copolymers. The experiments were conducted at 40 °C. At this rather high temperature and with the shear forces applied in the columns, association affects are not observed. The peaks, before and after the functionalization reactions, were identical in terms of the molecular weight distribution and the apparent molecular weight. Therefore, it is obvious that the functionalization reactions do not affect the molecular characteristics of the samples.

The results from low-angle laser light scattering (LALLS) in *n*-decane are given in Table 2 for the unfunctionalized and the corresponding functionalized copolymers. The aggregation numbers (N_w), defined as the ratio of the weight-average molecular weight of the samples in *n*-decane to that of the unfunctionalized diblocks in THF, are also incorporated in Table 2.

It is evident that micelles are formed in *n*-decane, which is selective solvent for the PI blocks. The aggregation numbers (N_w) are comparable for the unfunctionalized and the hydroxyl-

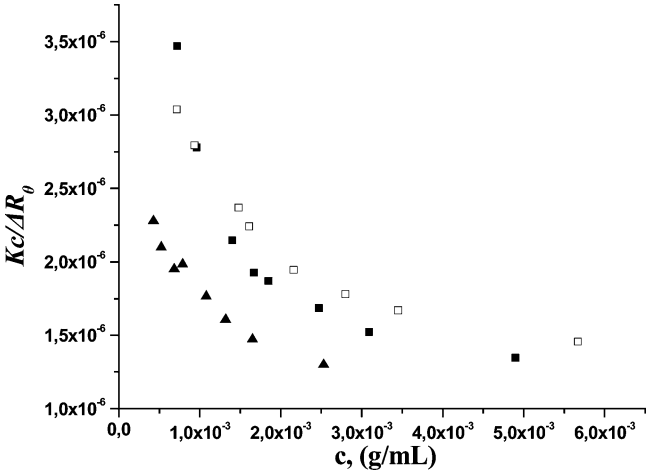

Figure 1. $Kc/\Delta R_\theta$ vs concentration plots for samples (■) IS 30/70, (□) ISOH 30/70 and (▲) ISUPy 30/70 in *n*-decane at 25 °C.

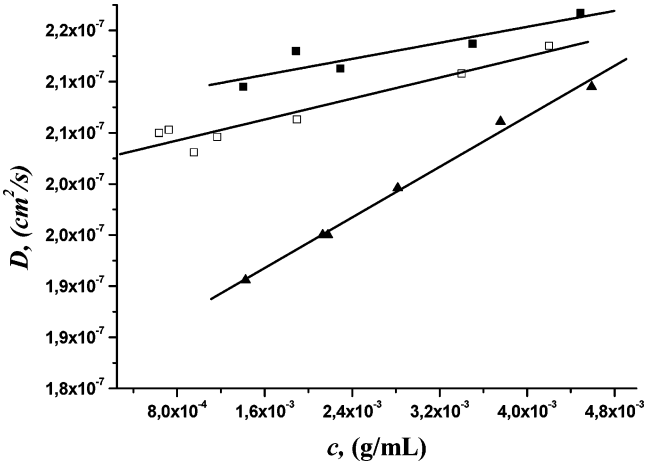

Figure 2. Diffusion coefficient vs concentration plots for samples (▲) IS 30/70, (■) ISOH 30/70, and (□) ISUPy 30/70 in *n*-decane at 25 °C.

functionalized samples with the same composition and increase upon increasing the molecular weight of the PS chain, which is the core forming block. The presence of the hydroxyl end groups, either at the PS or the PI block, does not affect appreciably the aggregation numbers compared to the unfunctionalized precursor diblock. Therefore, the hydroxyl groups are not capable of promoting further association in *n*-decane. The situation is different with the UPy functions. When they are located at the PS block (ISUPy samples) the same behavior is obtained as in the cases of the unfunctionalized diblocks. However, when the UPy groups are placed at the PI chains, the corona forming blocks, a much more extended association is obtained. The intensity of the scattered light is so big that accurate measurements of the molecular weights in *n*-decane cannot be obtained. This behavior can be attributed to the development of intermicellar interactions through the formation of hydrogen bonds between the UPy groups, which are located at the corona of the micelles. The formation of stable hydrogen bonds is favored in the nonpolar solvent, where the micelles are constructed. To confirm this behavior, the SIUPy samples were dissolved in *N*,*N*-dimethylacetamide, which is selective for the PS blocks. In this case the core consists of the PI chains and the unfunctionalized PS chains are the corona. Using the same concentrations as in the *n*-decane solutions, the scattered light intensity decreased to the normal values for micellar solutions.

Characteristic $Kc/\Delta R_\theta$ vs c plots are displayed in Figure 1. The critical micelle concentration (cmc) cannot be observed in all cases. Probably, the cmc is very low for all the systems and out of the experimentally accessible concentration range for light scattering measurements.

All the second virial coefficients are negative in *n*-decane, due to the decreased thermodynamic interactions between the polymeric chains and the solvent in the micellar solutions.

The static light scattering results were further confirmed by dynamic light scattering measurements. Table 3 displays the results for the ISOH and ISUPy diblock copolymers. In these samples the functional groups are attached to the core forming block.

The increased R_h values confirm the existence of micelles in the selective solvent *n*-decane. The concentration dependence of the apparent diffusion coefficient was linear in both the good, THF, and the selective solvent, *n*-decane. Representative plots are given in Figure 2. CONTIN analysis revealed that there is only one population in solution corresponding to micellar structures. The polydispersity factor μ_2/Γ^2, where Γ is the decay rate of the correlation function and μ_2 the second moment of the cumulant analysis, is always lower than 0.1, indicating the presence of monodisperse micellar structures. Angular or thermal dependence were not observed in *n*-decane for both the unfunctionalized and the functionalized copolymers leading to the conclusion that spherical and thermally stable micelles are formed.

Table 3. DLS Results for the IS Diblock Copolymers in THF and *n*-Decane at 25 °C

	THF			*n*-decane		
sample	$D_0 \times 10^7$ ($cm^2 \cdot s^{-1}$)	k_D ($mL \cdot g^{-1}$)	R_h (nm)	$D_0 \times 10^7$ ($cm^2 \cdot s^{-1}$)	k_D ($mL \cdot g^{-1}$)	R_h (nm)
IS 68/32	10.1	25.1	4.7	1.64	−16.5	15.5
ISOH 68/32				1.80	−21.4	14.1
ISUPy 68/32				1.75	−11.0	14.5
IS 52/48	8.87	45.2	5.4	1.82	−9.2	13.9
ISOH 52/48				2.27	11.5	11.1
ISUPy 52/48				1.99	2.2	12.8
IS 30/70	12.5	25.4	3.8	1.82	34.0	13.9
ISOH 30/70				2.10	7.0	12.1
ISUPy 30/70				2.04	4.4	12.4

It is obvious form the data given in Table 3 that there is a reduction of the hydrodynamic radius for the functionalized diblock copolymers compared to their unfunctionalized precursors. When hydroxyl is the functional group the reduction is more pronounced than the case of the UPy unit. The reduction in size is much higher than the experimental error of the method and systematic for all the samples. This behavior can be attributed to the presence of the functional groups, which modify the organization and the compactness of the micellar core. Polymeric chains interact through the formation of hydrogen bonds and the core becomes more compact. This phenomenon is more pronounced in the case of the hydroxyl group, since it is smaller than the UPy unit and can interact with two other groups (Scheme 2). Consequently, steric hindrance effects are negligible, allowing for a better organization of the core and therefore, lower R_h values.

The DLS results from the samples SI, SIOH, and SIUPy are given in Table 4. For these polymers, the functional groups are attached to the polyisoprene block, which forms the corona of the micelles. Consequently, they are located at the outer shell of the micelles.

In the case of the unfunctionalized precursors CONTIN analysis revealed the presence of micellar structures in *n*-decane. The micelles are near monodisperse, since the μ_2/Γ^2 ratio is lower than 0.1 and spherical, since an angular dependence of

Scheme 2. Micellar Structures Formed from the IS, ISOH, and ISUPy Block Copolymers in *n*-Decane[a]

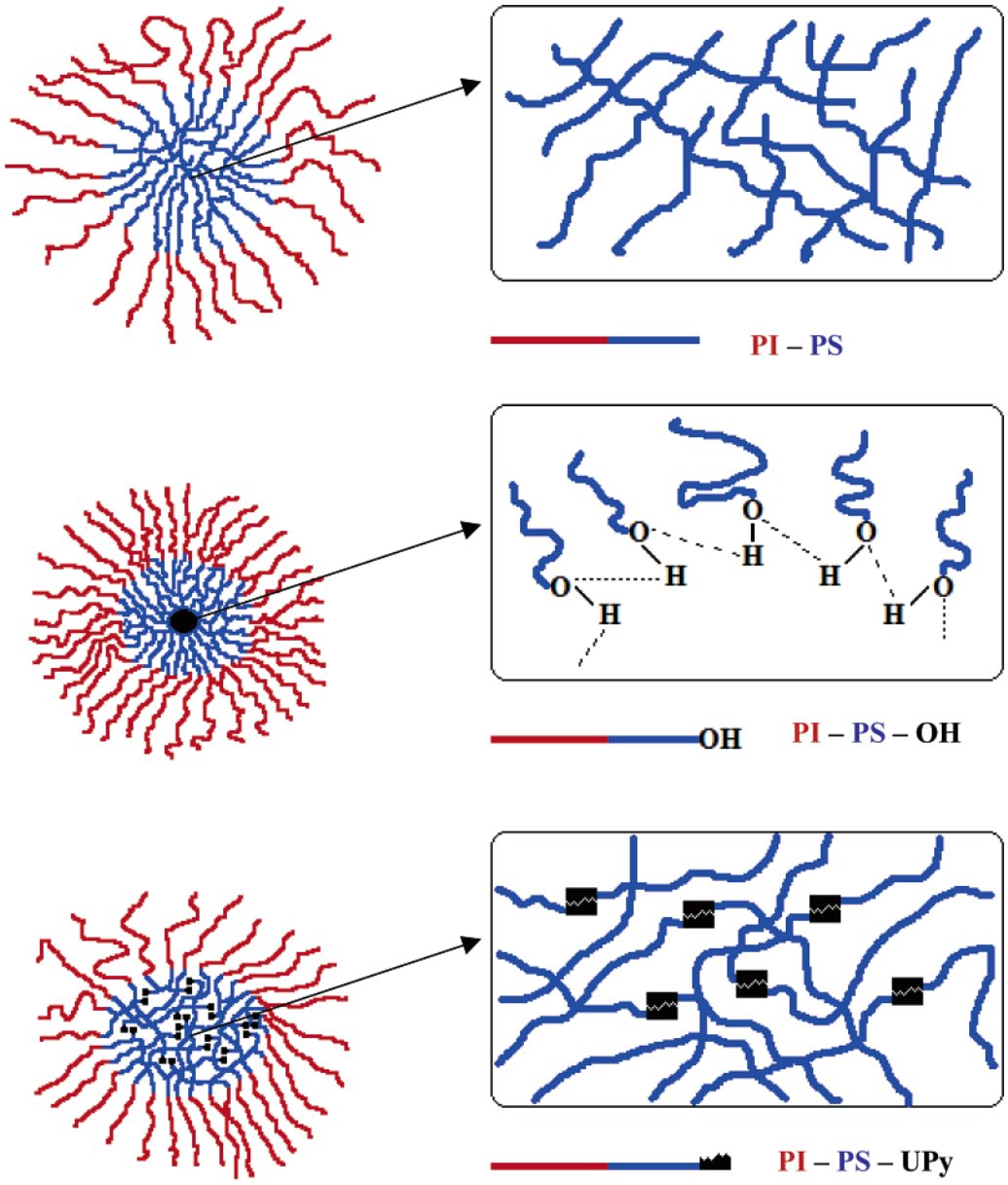

[a] The conformation of the core is given in the inset.

Table 4. DLS Results for the SI Diblock Copolymers in THF and *n*-Decane at 25 °C

	THF			*n*-decane					
				$D_0 \times 10^7$ ($cm^2 \cdot s^{-1}$)		k_D ($mL \cdot g^{-1}$)		R_h (nm)	
sample	$D_0 \times 10^7$ ($cm^2 \cdot s^{-1}$)	k_D ($mL \cdot g^{-1}$)	R_h (nm)	1st population	2nd population	1st population	2nd population	1st population	2nd population
SI 33/67	10.5	25.8	4.5	22.7		0.5		11.2	
SIOH 33/67				25.6	5.82	382.4	54.0	9.9	43.6
SIUPy 33/67				27.9	4.92	5.9	148.0	9.1	51.5
SI 46/54	9.75	33.5	4.8	21.3		43.7		11.9	
SIOH 46/54				31.5	3.61	93.0	14.3	8.1	70.3
SIUPy 46/54				30.0	3.06	122.7	83.3	8.5	82.9
SI 64/36	3.92	61.2	6.5	17.3		94.2		14.6	
SIOH 64/36				18.1	1.76	40.7	670.5	14.0	144.1
SIUPy 64/36				15.6	1.94	53.6	439.7	16.2	130.8

the R_h values was not observed.[61] Moreover, thermal treatment up to 55 °C showed that the micelles are thermally stable.

A different situation is obtained for the functionalized diblock copolymers. CONTIN analysis confirmed the presence of a bimodal distribution in *n*-decane. The first population does not show any angular dependence, is monodisperse and thermally stable up to 55 °C. Therefore, it corresponds to micelles. The second population is polydisperse ($\mu_2/\Gamma^2 > 0.2$) and shows intense angular dependence. Consequently, the measurements were conducted at seven different angles from 45° to 135° and the diffusion coefficient was obtained from the slope of the Γ/q^2 vs q plot. The percentage of the second population varies

Scheme 3. Shrinkage of the Micellar Structures of the SIUPy Micelles Compared to the Corresponding SI Micelles

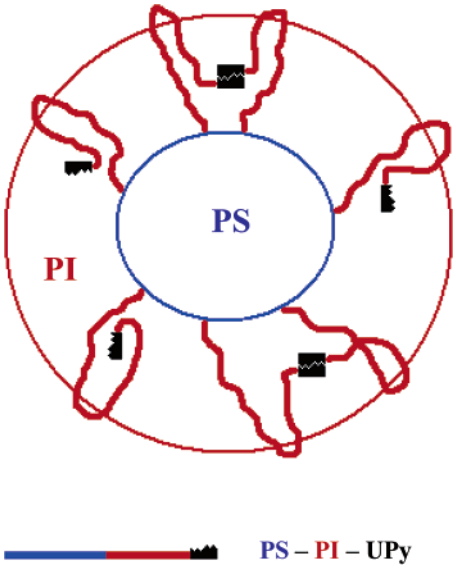

between 5 and 10% for the hydroxyl-functionalized diblocks and between 10 and 20% for the UPy terminated samples. Furthermore, for the same sample the percentage of the second population increases by increasing the concentration. At very high concentrations gels were obtained for the UPy-functionalized diblocks. The low amount of clusters and the lower concentrations used for the static light scattering measurements confirm the low aggregation numbers found by LALLS in the case of the hydroxyl-functionalized polymers.

According to these results equilibrium between micelles and clusters is established in *n*-decane solutions of the functionalized samples. The clusters are formed due to the incompatibility of the polar functional groups with the nonpolar solvent. Therefore, the functional groups interact with each other through the formation of hydrogen bonds leading to the formation of intermicellar structures. This effect is more pronounced in the case of the UPy-functionalized polymers, due to the formation of the much more stable four hydrogen bonds array between two different UPy groups, compared to the samples bearing hydroxyl end groups. The same interactions of the functional groups are responsible for the reduced size of the micellar structures (first population, Table 4) obtained from the end-functionalized copolymers compared to the micelles obtained from the unfunctionalized diblocks. The reduction of the micellar R_h values varies between 11 to more than 30% and generally is more pronounced for the UPy-terminated samples. The corona of the micelles shrinks, due to the formation of intramicellar hydrogen bonds between different functional groups, which are located to the same corona (Scheme 3). Only in the case of sample SIUPy 64/36 there is a deviation from this behavior. It does not seem to be an experimental error, since the measurement was repeated. Consequently, this behavior indicates a system with less extended intramolecular hydrogen bonds, and the behavior can be attributed to the higher aggregation number and the lower molecular weight of the PI block. Therefore, for the specific sample the PI chains are more stretched than for the other samples with lower aggregation numbers. Consequently, the chain folding for the intramicellar interaction of the UPy groups is less probable.

The thermal stability of the intermicellar structures was examined by DLS measurements. In Figure 3, R_h vs temperature plots are given for the SIOH 33/67 and SIUPy 33/67 diblock

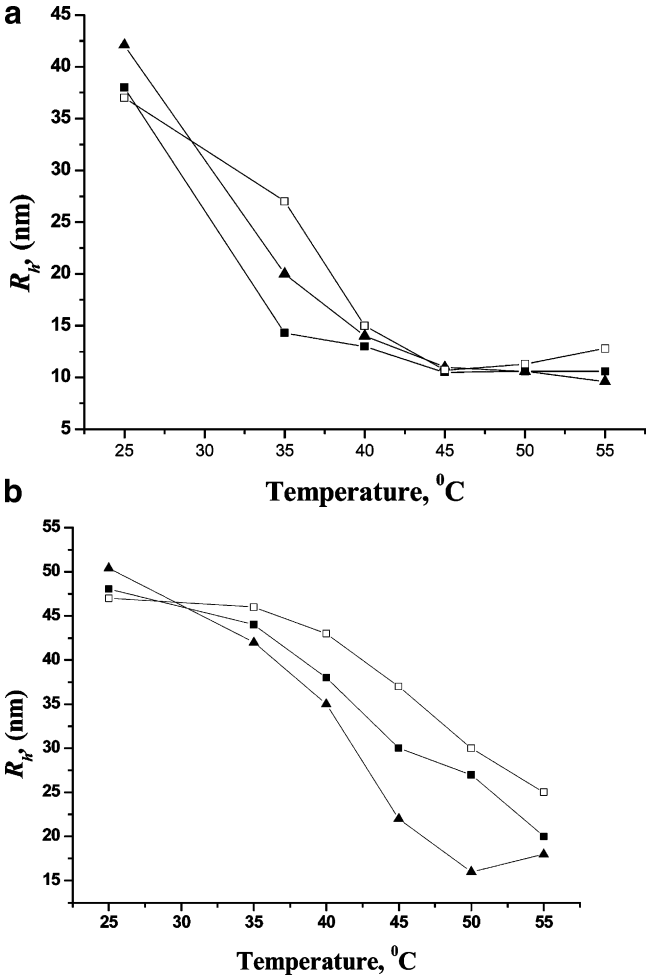

Figure 3. (a) R_h vs temperature plots for sample SIOH 33/67 (▲) $c = 9.363 \times 10^{-4}$ g/mL, (■) $c = 4.261 \times 10^{-3}$ g/mL, and (□) $c = 8.522 \times 10^{-3}$ g/mL. (b) Same plots for sample SIUPy 33/67 (▲) $c = 9.256 \times 10^{-4}$ g/mL, (■) $c = 4.832 \times 10^{-3}$ g/mL, and (□) $c = 8.220 \times 10^{-3}$ g/mL.

copolymers. The measurements were conducted using different concentrations at six temperatures from 25 to 55 °C.

At 25 °C there is equilibrium between micelles and clusters. By increasing the temperature the intermicellar structures are almost totally destroyed so that at higher temperatures mainly micelles exist in solution. The micellar size (first population) for samples SIOH 33/67 and SIUPy 33/67 at 25 °C is 9−10 nm. The second population (intermicellar aggregates) have R_h values around 40−50 nm at 25 °C. By increasing the temperature these values are substantially decreased to 10−15 nm. Taking into account the possible expansion of the corona chains by increasing the temperature, it is reasonable to assume that almost all the clusters are disrupted, because the energy provided to the system by increasing the temperature is capable to disrupt the hydrogen bonds formed by the functional end groups. For sample SIOH 33/67 the plateau with constant R_h values is achieved at lower temperatures (around 45 °C) than sample SIUPy 33/67, due to the weaker interactions of the hydroxyl groups. The four hydrogen bonds developed for each pair of UPy groups offer a better stability. For the lower concentration curve it is obvious that even for the UPy functionalized sample the plateau is reached at 50−55 °C. For the higher concentration curves, this region is not experimentally accessible, due to the instrumental limitations in working at higher temperatures. The higher the concentration the slower is the rate of destruction of the clusters, due to the increased number of hydrogen bonds

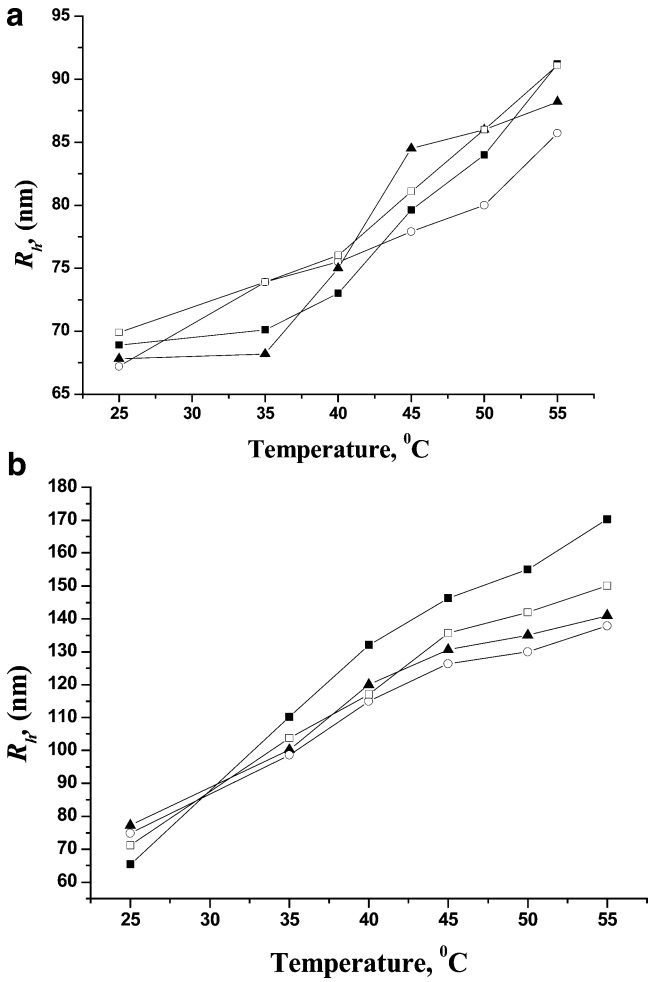

Figure 4. (a) R_h vs temperature plots for sample SIOH 46/54 (○) $c = 1.326 \times 10^{-3}$ g/mL, (▲) $c = 2.465 \times 10^{-3}$ g/mL, (■) $c = 4.351 \times 10^{-3}$ g/mL, and (□) $c = 7.742 \times 10^{-3}$ g/mL. (b) Same plots for sample SIUPy 46/54 (▲) $c = 4.896 \times 10^{-4}$ g/mL, (○) $c = 1.006 \times 10^{-3}$ g/mL, (□) $c = 4.211 \times 10^{-3}$ g/mL, and (■) $c = 7.624 \times 10^{-3}$ g/mL.

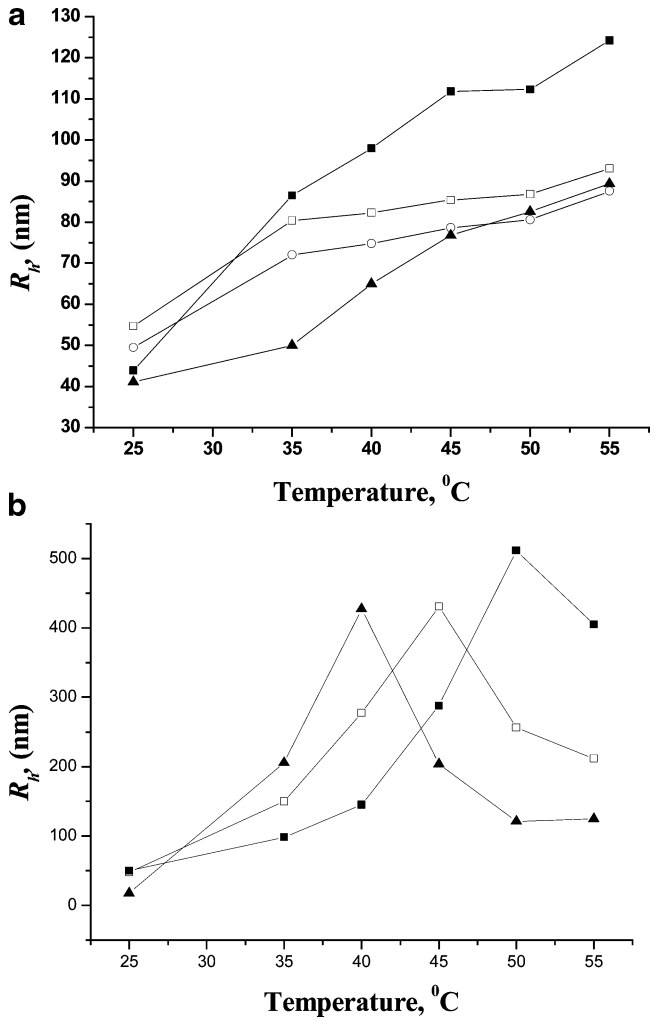

Figure 5. (a) R_h vs temperature plots for sample SIOH 64/36 (○) $c = 1.019 \times 10^{-3}$ g/mL, (□) $c = 3.956 \times 10^{-3}$ g/mL, (▲) $c = 5.001 \times 10^{-3}$ g/mL, and (■) $c = 7.759 \times 10^{-3}$ g/mL. (b) Same plots for sample SIUPy 64/36 (▲) $c = 4.111 \times 10^{-3}$ g/mL, (□) $c = 5.356 \times 10^{-3}$ g/mL, and (■) $c = 8.997 \times 10^{-3}$ g/mL.

that have to be disrupted at higher concentrations. Another parameter contributing to the instability of the intermicellar structures is the fact that the specific sample has the highest molecular weight of the PI block. Therefore, the effect of the end group is minimized.

In Figures 4 and 5, the variation of R_h with temperature is depicted for the functionalized SI 46/54 and SI 64/36 diblock copolymers.

A different behavior was evidenced for these samples. The increase of temperature leads to clusters with much higher R_h values. Furthermore, the equilibrium is shifted in favor of the clusters. The effect is much more pronounced for the UPy-terminated copolymers (Scheme 4). For these samples the degree of association is higher than for the SI 33/67 copolymers. Therefore, each micelle has a higher number of functional groups at the corona. Consequently, the number of interacting groups between the different micelles is higher for the SI 46/54 and SI 64/36 copolymers. Furthermore, for these samples the PI block has lower molecular weight. Thus, the contribution of the functional end group is more pronounced in this case. For sample SIUPy 64/36 a tremendous increase of the clusters' R_h values was observed, leading to a maximum size. After that the clusters are disrupted to smaller structures. The disruption is not so intense to form simple micelles. The maximum cluster R_h value is shifted to higher temperature by increasing the concentration of the copolymer.

The general behavior of the samples is the same. The introduction of the functional end groups at the corona forming blocks induces strong intermicellar interactions leading to the formation of clusters. However, the nature of the equilibrium between micelles and clusters and its dependence from the temperature seems to be very delicate and depends on several parameters, as the nature of the end group, the molecular weight and the composition of the block copolymers, the degree of association of the micelles, the micellar concentration etc. It is evident that for micelles having lower aggregation numbers and a higher molecular weight of the corona-forming block the interactions between the end groups are not so strong. More stable structures are formed at lower temperatures. For samples with higher aggregation numbers and lower molecular weight of the corona forming block, the increase of temperature facilitates the development of intermicellar interactions leading to the formation of larger clusters. It is obvious that more samples have to be studied in order to further clarify the temperature dependence of the aggregation behavior of these materials.

Viscometry measurements were also performed. The results are given in Table 5, and representative plots are displayed in Figure 6.

The existence of micelles is confirmed from the increased R_v values in *n*-decane, compared to those obtained in THF. The

Scheme 4. Effect of the Temperature on the Equilibrium between Micelles and Intermicellar Clusters for the SIUPy Samples

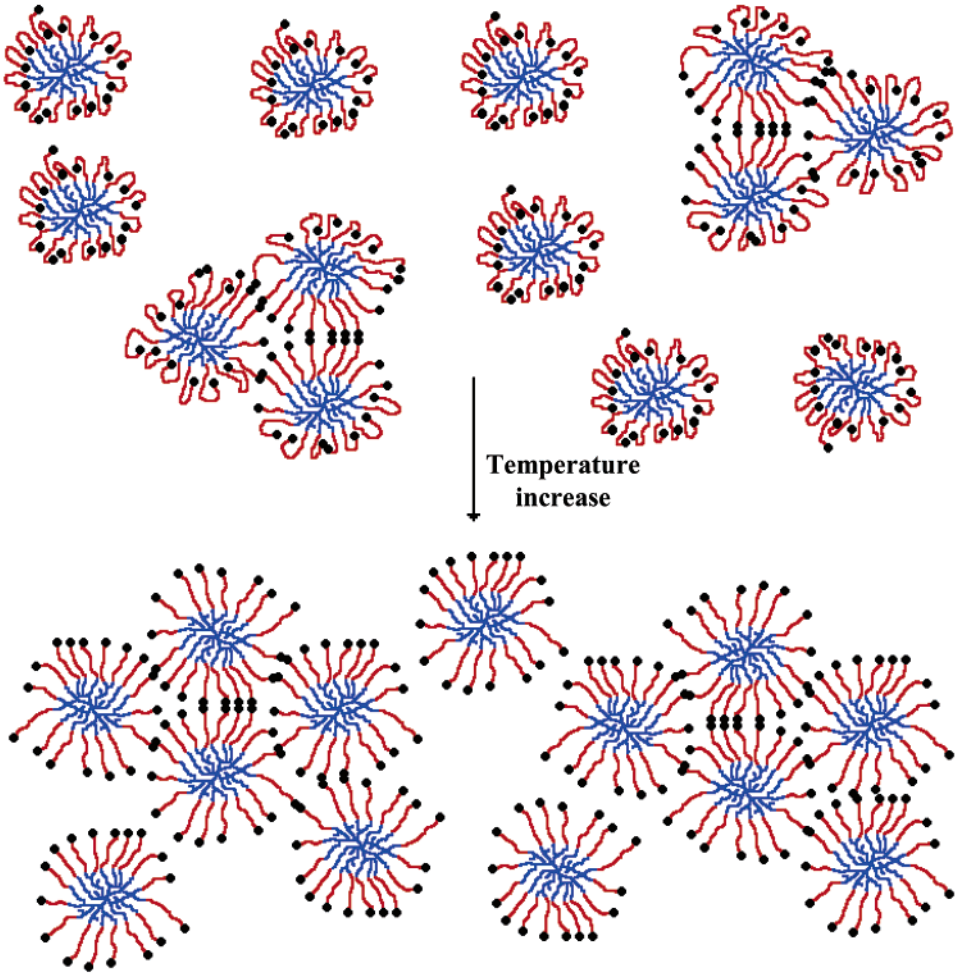

Table 5. Viscometry Results for the Diblock Copolymers in THF, *n*-Decane and $CHCl_3$ at 25 °C

	THF			*n*-decane					$CHCl_3$		
sample	$[\eta]$ (dL·g^{-1})	k_H	R_v (nm)	$[\eta]$ (dL·g^{-1})	k_H	R_v (nm)	R_h[a] (nm)	R_v/R_h	$[\eta]$ (dL·g^{-1})	k_H	R_v (nm)
SI 33/67	0.169	0.40	3.0	0.124	0.67	5.9	11.2	0.53			
SIOH 33/67											
SIUPy 33/67											
SI 46/54	0.159	0.34	3.1								
SIOH 46/54				0.098	1.2	6.7	8.1	0.83			
SIUPy 46/54				0.109	0.93				0.185	0.40	5.6
SI 64/36	0.138	0.49	3.8	0.062	2.2	10.2	14.6	0.70	0.159	0.29	3.9
SIOH 64/36				0.067	2.2	10.7	14.0	0.76			
SIUPy 64/36 (25 °C)				0.072	2.4				0.153	0.43	
SIUPy 64/36 (40 °C)				0.092	0.25						
SIUPy 64/36 (45 °C)				0.088	0.28						
IS 30/70	0.125	0.51	2.9	0.071	1.3	8.1	13.9	0.58		0.66	
ISOH 30/70				0.072	1.1	8.2	12.1	0.68			
ISUPy 30/70				0.071	1.3	8.2	12.4	0.66	0.134	0.60	
IS 52/48	0.144	0.63	3.0	0.110	0.95	7.0	13.9	0.50			
ISOH 52/48											
ISUPy 52/48									0.151	0.44	4.8
IS 68/32	0.166	0.83	3.1								
ISOH 68/32				0.128	0.69	6.5	14.1	0.46			
ISUPy 68/32											

[a] By differential light scattering (DLS) in *n*-Decane.

high values of the Huggins coefficients, due to increased hydrodynamic interactions of the polymeric chains in the aggregates, lead to the same conclusion. It is observed that the R_v values are always lower than the corresponding R_h values. This behavior can be attributed to the higher sensitivity of dynamic light scattering to the larger micellar structures (D is a z-average quantity) and/or the development of shear forces in the capillary viscometer which may disrupt the micellar aggregates. This behavior has been previously obtained in micellar and aggregating systems.[62,63] The intermicellar aggregates, which are formed through the hydrogen bonds formation between the micellar structures are more susceptible to disrup-

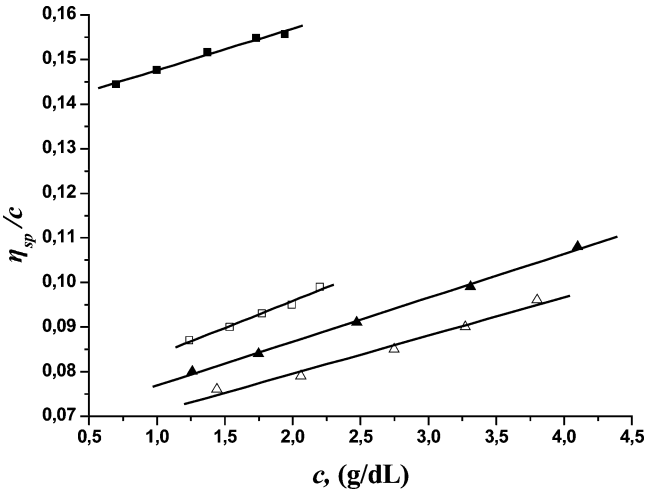

Figure 6. Viscometry plots for samples (■) SI 64/36 in THF at 25 °C, (○) SI 64/36, (▲) SIOH 64/36, and (□) SIUPy 64/36 in *n*-decane at 25 °C.

tion in the viscometer's capillary tube. However, as it is evident from the unfunctionalized samples even the simple micelles may be disassociated by the shear forces of the viscometry tube.

The intrinsic viscosity is always lower in *n*-decane than in THF. Comparing this result with the higher R_v values obtained in the selective solvent it is concluded that the micelles are more compact than the free copolymeric chains in THF, which is a common good solvent for all the blocks.

From the samples of the IS 30/70 series, it is evident that the end-functionalized copolymers display higher stability in the viscometer tube, showing a lower reduction of the R_v values in comparison to the corresponding R_h values. This behavior can be attributed to the presence of the hydrogen bonds that are developed in the micellar core. Consequently, higher amounts of energy are needed to disrupt the hydrogen bonds and then lead to deaggregation of the micelles.

By comparison of the intrinsic viscosities of samples SIOH 46/54 and SIUPy 46/54 as well as of samples SIOH 64/36 and SIUPy 64/36, it is obvious that the intrinsic viscosity values are higher for the UPy-functionalized samples than for the hydroxyl-terminated ones. This is direct evidence of the more extended intermicellar aggregates in the first case. Furthermore, the formation of four hydrogen bonds between two UPy groups makes the clusters more stable compared to those formed by the hydroxyl-functionalized copolymers.

The intrinsic viscosity of the sample SIUPy 64/36 was also measured at 40 and 45 °C in *n*-decane (Table 5). It was observed that the intrinsic viscosity increases from 0.072 dL/g at 25 °C to 0.092 dL/g at 40 °C and then slightly reduces to 0.088 dL/g at 45 °C. These results indicate that the increase of temperature facilitates the formation of large clusters through the formation of intermicellar hydrogen bonds between the UPy groups. The shear forces applied in the viscometer tube are strong enough to disrupt the hydrogen bond interactions, therefore allowing for the formation of clusters. At temperatures higher than 40 °C the clusters start decomposing to smaller structures. The same behavior was obtained by DLS measurements.

The ability of the UPy groups to associate was further tested by conducting static light scattering and viscometry experiments in $CHCl_3$, a common good solvent for both the PS and PI blocks. The LALLS measurements were performed for samples SIUPy 46/54 and ISUPy 52/48 (Table 6). It is obvious that the polymers associate in $CHCl_3$, due to the formation of hydrogen bonds between the UPy groups. Meijer et al. reported the formation of dimers in solution and in the solid state for polymers end-functionalized with the UPy groups. However, Long et al. confirmed the presence of extended aggregation for end-functionalized PS and PI polymers with UPy groups in the solid state. The same association behavior was also obtained for polyacrylate chains containing 10 mol % UPy groups along the polymer backbone in nonpolar solvents, such as toluene and $CHCl_3$.

Table 6. LALLS Results for the Functionalized Diblock Copolymers SIUPy 46/54 and ISUPy 52/48 in $CHCl_3$ at 25 °C

sample	$\overline{M_w} \times 10^{-3}$	$A_2 \times 10^3$ mL·mol·g^{-2}	d*n*/d*c*,[b] mL·g^{-1}	N_w[a]
SIUPy 46/54	58.6	1.30	0.128	5
ISUPy 52/48	47.8	6.76	0.126	4

[a] Weight-average degree of association. [b] By differential refractometry in $CHCl_3$ at 25 °C.

Table 7. DSC Results for Unfunctionalized and Functionalized Diblock Copolymers

sample	T_{g1} (°C)	ΔT_{g1} (°C)	T_{g2} (°C)	ΔT_{g2} (°C)
SI 33/67	−59.77		54.58	
SIOH 33/67	−56.83	2.94	54.16	−0.42
SIUPy 33/67	−53.35	6.42	55.71	1.13
SI 46/54	−57.94		47.39	
SIOH 46/54	−56.08	1.86	48.67	1.28
SIUPy 46/54	−54.99	2.95	48.75	1.36
SI 64/36	−56.24		48.89	
SIOH 64/36	−52.41	3.83	49.71	0.82
SIUPy 64/36	−50.67	5.57	50.13	1.24
IS 30/70	−58.35		43.98	
ISOH 30/70	−58.48	−0.13	47.00	3.02
ISUPy 30/70	−58.69	−0.34	49.60	5.62
IS 52/48	−59.66		47.25	
ISOH 52/48	−59.16	0.50	49.57	2.32
ISUPy 52/48	−60.82	−1.16	54.83	7.58
IS 68/32	−59.46		52.63	
ISOH 68/32	−59.34	0.12	53.30	0.67
ISUPy 68/32	−59.01	0.45	55.79	3.16

Viscometry data on selected samples are presented in Table 5. The higher intrinsic viscosities of the unfunctionalized samples than in THF indicate that $CHCl_3$ is a better solvent than THF for the specific samples. Comparing the results of the unfunctionalized with the corresponding UPy-functionalized copolymers it is obvious that the intrinsic viscosity remains almost unchanged indicating that the associates are completely disrupted due to the shear forces applied in the viscometer tube.

Further evidence regarding the presence of hydrogen bonds in the solid state were provided by differential scanning calorimetry (DSC) and thermogravimetric analysis (TGA). The glass transition temperatures, T_g, of the diblock copolymers were calculated by the DSC measurements. Table 7 summarizes the results from all the samples.

Literature data regarding linear PS and PI samples, having similar molecular weights with the examines samples, reveal that the expected T_g values for the two blocks are ∼+70 and ∼ −65 °C for the PS and PI blocks, respectively. Table 7 shows that for the unfunctionalized copolymers two different T_g values are obtained, indicating that the copolymers are microphase separated. However, the T_g of the PI block is shifted to higher values, whereas the T_g of the PS block to lower values, revealing partial mixing of the two blocks. The functionalized copolymers possess two different T_gs as well. The T_g of the block that does not carry the functional group hardly changes compared to the unfunctionalized copolymer. However, the T_g of the block which carries the functional group increases appreciably. The effect is much more pronounced for the UPy-terminated samples, compared to the hydroxyl-functionalized copolymers. The effect

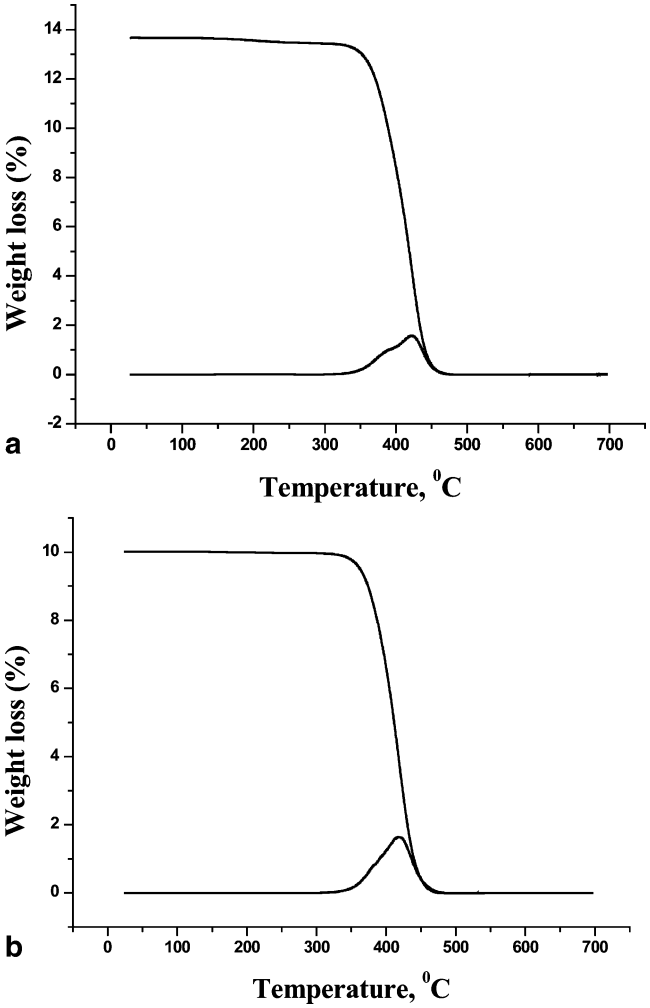

Figure 7. Decomposition procedures for samples (a) ISUPy 30/70 and (b) SIUPy 64/36.

Table 8. TGA Results for the Series of SI 64/36 and IS 30/70 Diblock Copolymers

sample	dec temp at the max wt loss (°C)		temp range of dec (°C)
SI 64/36	416.72		333.41−476.27 (142.86)
SIOH 64/36	417.23		326.24−475.32 (149.08)
SIUPy 64/36	417.22		326.60−478.60 (152.00)
IS 30/70	424.79	396.65	335.50−471.53 (136.03)
ISOH 30/70	421.43	393.63	325.38−468.15 (142.77)
ISUPy 30/70	422.11	393.63	316.82−468.33 (151.51)

is attributed to the presence of the end groups interactions, through the formation of hydrogen bonds. These interactions are stronger between the UPy units and reduce the mobility of the functionalized block segments. The relatively low molecular weight of the blocks allows for a significant contribution of the end group. This effect has been previously shown for linear homopolymers and block copolymers having functional end groups.

The same conclusions are reached from the TGA results, which are incorporated in Table 8. Two decomposition procedures are evident for the series of IS 30/70 diblock copolymers. The thermal decomposition of the PI block (∼394 °C) is initially observed, followed by the decomposition of the PS block (∼422 °C), as is shown in Figure 7a.

The decomposition temperatures at the maximum weight loss for the PS and the PI homopolymers are 426 and 380 °C, respectively. The first transition appears as a shoulder, due to the low amount of PI block and that two thermal events take place at similar temperatures. In the case of the diblock copolymers of the SI 64/36 series, the two distinct decomposition temperatures are not observed. The functional group is located at the PI chain end. Therefore, the decomposition temperature range for the PI block becomes broader, due to the increased thermal stability offered by the functional group and consequently, cannot be distinguished from the decomposition of the PS block (Figure 7b). The incorporation of a functional group does not affect the maximum decomposition temperature but the temperature range of the thermal decomposition. This phenomenon is more pronounced in the case of the UPy functionalized samples due to the stronger intermolecular noncovalent interactions. Extra thermal energy is required to disrupt the hydrogen bonds and possible aggregation structures.

Conclusions

The existence of a dynamic system was confirmed for the series of ω-functionalized diblock copolymers in solution carrying 2-ureido-4-pyrimidinone (UPy) groups. The combination of two reversible phenomena, micellization and secondary interactions (hydrogen bonding), created a complex system having properties which depended on the chemical environment, temperature, concentration and nature of solvent, in which the unimers (ω-functionalized diblock copolymers) are dissolved. The effect of functional groups on micellization is different depending on their position in formed micelles and their association power by hydrogen bonds. The reversibility of their properties specifies the flexibility of these unimers and it is not overstatement to describe them as "clever materials".

Acknowledgment. The financial support of the Ministry of Education through the Program "Polymer Science and its Applications" and the Research Committee of the University of Athens through the program Kapodistrias is greatly acknowledged.

References and Notes

(1) Lehn, J.-M. *Supramolecular Chemistry, Concepts and Perspectives*; VCH Weinheim, Germany, 1995.
(2) Dietrich, B.; Lehn, J.-M.; Sauvage, J.-P. *Tetrahedron Lett.* **1969**, *10*, 2889.
(3) Dietrich, B.; Lehn, J.-M.; Sauvage, J.-P.; Blanzat, J. *Tetrahedron* **1973**, *29*, 1629.
(4) Dietrich, B.; Lehn, J.-M.; Sauvage, J.-P. *Tetrahedron* **1973**, *29*, 1647.
(5) Pedersen, C. J. *J. Am. Chem. Soc.* **1976**, *89*, 7017.
(6) Pedersen, C. J. *Angew. Chem., Int. Ed. Engl.* **1988**, *27*, 1053.
(7) Cram, D. J.; Cram, J. M. *Science* **1974**, *183*, 803.
(8) Sijbesma, R. P.; Meijer, E. W. *Curr. Opin. Colloid Interface Sci.* **1999**, *4*, 24.
(9) ten Cate, A. T.; Sijbesma, R. P. *Macromol. Rapid Commun.* **2002**, *23*, 1094.
(10) Sijbesma, R. P.; Meijer, E. W. *Chem. Commun.* **2003**, 5−16.
(11) Beijer, F. H.; Kooijiman, H.; Spek, A. L.; Sijbesma, R. P.; Meijer, E. W. *Angew. Chem., Int. Ed. Engl.* **1998**, *37*, 75.
(12) Jørgensen, W. L.; Pranata, J. *J. Am. Chem. Soc.* **1990**, *112*, 2008.
(13) Brunsveld, L.; Folmer, J. B.; Meijer, E. W.; Sijbesma, R. P. *Chem. Rev.* **2001**, *101*, 4071.
(14) Beijer, F. H.; Sijbesma, R. P.; Vekemans, J. A. J. M.; Meijer, E. W.; Kooijiman, H.; Spek, A. L. *J. Org. Chem.* **1996**, *61*, 6371.
(15) Murray, T. J.; Zimmerman, S. C. *J. Am. Chem. Soc.* **1992**, *114*, 4010.
(16) Hamilton, A. D.; Van Engen, D. *J. Am. Chem. Soc.* **1987**, *109*, 5035.
(17) Kyogoku, Y.; Lord, R. C.; Rich, A. *Biochim. Biophys. Acta* **1969**, *179*, 10.
(18) Fenlon, E. E.; Murray, T. J.; Baloga, M. H.; Zimmerman, S. C. *J. Org. Chem.* **1993**, *58*, 6625.
(19) Murray, T. J.; Zimmerman, S. C.; Kolotuchin, S. V. *Tetrahedron* **1995**, *51*, 635.
(20) Zimmerman, S. C.; Murray, T. J. *Tetrahedron Lett.* **1995**, *36*, 7627.
(21) Schmuck, C.; Wienand, W. *Angew. Chem., Int. Ed. Engl.* **2001**, *40*, 4363.

(22) Zeng, H.; Miller, R. S.; Flowers, R. A.; Gong, B. *J. Am. Chem. Soc.* **2000**, *122*, 2635.
(23) Folmer, B. J. B.; Sijbesma, R. P.; Kooijiman, H.; Spek, A. L.; Meijer, E. W. *J. Am. Chem. Soc.* **1999**, *121*, 9001.
(24) Yang, X.; Hua, F.; Yamato, K.; Ruckenstein, E.; Gong, B.; Kim, W.; Ryu, C. Y. *Angew. Chem., Int. Ed.* **2004**, *43*, 6471.
(25) Kunz, M. J.; Hayn, G.; Saf, R.; Binder, W. H. *J. Polym. Sci., Polym. Chem. Ed.* **2004**, *42*, 661.
(26) Binder, W. H.; Bernstorff, S.; Kluger, C.; Petraru, L.; Kunz, M. J. *Adv. Mater.* **2005**, *17*, 2824.
(27) Binder, W. H.; Kunz, M. J.; Ingolic, E. *J. Polym. Sci., Polym. Chem. Ed.* **2004**, *42*, 162.
(28) Gohy, J.-C.; Lohmeijer, B. G. G.; Schubert, U. S. *Chem.—Eur. J.* **2003**, *9*, 3472.
(29) Gohy, J.-C.; Lohmeijer, B. G. G.; Alexeev, A.; Wang, X.-S.; Manners, I. Winnik, M. A.; Schubert, U. S. *Chem.—Eur. J.* **2004**, *10*, 4315.
(30) Gohy, J.-C.; Lohmeijer, B. G. G.; Schubert, U. S. *Macromolecules* **2002**, *35*, 4560.
(31) Gohy, J.-C.; Lohmeijer, B. G. G.; Varshney, S. K.; Schubert, U. S. *Macromolecules* **2002**, *35*, 7427.
(32) Gohy, J.-C.; Lohmeijer, B. G. G.; Varshney, S. K.; Décamps, B.; Leroy, E.; Boileau, S.; Schubert, U. S. *Macromolecules* **2002**, *35*, 9748.
(33) Gohy, J.-C.; Lohmeijer, B. G. G.; Schubert, U. S. *Macromol. Rapid Commun.* **2002**, *23*, 555.
(34) Mayer, G.; Vogel, V.; Lohmeijer, B. G. G.; Gohy, J.-C.; Van den Broek, J. A.; Haase, W.; Schubert, U. S.; Schubert, D. *J. Polym. Sci., Polym. Chem. Ed.* **2004**, *42*, 4458.
(35) Gohy, J.-C.; Lohmeijer, B. G. G.; Décamps, B.; Leroy, E.; Boileau, S.; Van den Broek, J. A.; Schubert, D.; Haase, W.; Schubert, U. S. *Polym. Int.* **2003**, *52*, 1611.
(36) Gohy, J.-C.; Hofmeier, H.; Alexeev, A.; Schubert, U. S. *Macromol. Chem. Phys.* **2003**, *204*, 1524.
(37) Sijbesma, R. P.; Beijer, F. H.; Brunsveld, L.; Folmer, B. J. B.; Hirschberg, J. H. K. K.; Lange, R. F. M.; Lowe, J. K. L.; Meijer, E. W. *Science* **1997**, *278*, 1601.
(38) Söntjens, S. H. M.; Sijbesma, R. P.; van Genderen, M. H. P.; Meijer, E. W. *Macromolecules* **2001**, *34*, 3815.
(39) Kelly, J. R.; Maguire, M. P. *J. Am. Chem. Soc.* **1987**, *109*, 6549.
(40) Söntjens, S. H. M.; Sijbesma, R. P.; van Genderen, M. H. P.; Meijer, E. W. *J. Am. Chem. Soc.* **2000**, *122*, 7487.
(41) Beijer, F. H.; Sijbesma, R. P.; Kooijiman, H.; Spek, A. L.; Meijer, E. W. *J. Am. Chem. Soc.* **1998**, *120*, 6761.
(42) Folmer, B. J. B.; Sijbesma, R. P.; Versteegen, R. M.; van der Rijt, J. A. J.; Meijer, E. W. *Adv. Mater.* **2000**, *12*, 874.
(43) Yamauchi, K.; Lizotte, J. R.; Long, T. E. *Macromolecules* **2002**, *35*, 8745.
(44) Yamauchi, K.; Lizotte, J. R.; Hercules, D. M.; Vergne, M. J.; Long, T. E. *J. Am. Chem. Soc.* **2002**, *124*, 8599.
(45) Yamauchi, K.; Lizotte, J. R.; Long, T. E. *Macromolecules* **2003**, *36*, 1083.
(46) Yamauchi, K.; Kanomata, A.; Inoue, T.; Long, T. E. *Macromolecules* **2004**, *37*, 3519.
(47) McKee, M. G.; Elkins, C. L.; Park, T.; Long, T. E. *Macromolecules* **2005**, *38*, 6015.
(48) Riess, G. *Prog. Polym. Sci.* **2003**, *28*, 1107.
(49) Tuzar, Z.; Kratochvil, P. *Surf. Colloid Sci.* **1993**, *15*, 1.
(50) Price, C.; Chan, E. K. M.; Mobbs, R. H.; Stubberfield, R. B. *Eur. Polym. J.* **1985**, *21*, 355.
(51) Tuzar, Z.; Kratochvil, P. *Adv. Colloid Interface Sci.* **1976**, *6*, 201.
(52) Prochazka, K.; Delcros, H.; Delmas, G. *Can. J. Chem.* **1988**, *66*, 915.
(53) Nakano, M.; Matsuoka, H.; Yamaoka, H.; Poppe, A.; Richter, D. *Macromolecules* **1999**, *32*, 697.
(54) Zhao, J. Q.; Pearce, E. M.; Kwei, T. K.; Jeon, H. S.; Keseni, P. K.; Balsara, N. P. *Macromolecules* **1995**, *28*, 1972.
(55) Schillen, K.; Brown, W.; Johnsen, R. M. *Macromolecules* **1994**, *27*, 4825.
(56) Zhang, L.; Eisenberg, A. *Science* **1995**, *268*, 1728.
(57) Moffit, M.; Khougaz, K.; Eisenberg, A. *Acc. Chem. Res.* **1996**, *29*, 95.
(58) Zhulina, E. B.; Birnstein, O. V. *Polym. Sci. USSR* **1987**, *27*, 570.
(59) Hadjichristidis, N.; Iatrou, H.; Pispas, S.; Pitsikalis, M. *J. Polym. Sci., Polym. Chem.* **2000**, *38*, 3211.
(60) Reed, S. F., Jr. *J. Polym. Sci., Part A−1* **1972**, *10*, 1187.
(61) (a) Burchard, W. *Combined static and dynamic light scattering in Light Scattering. Principles and Development*; Brown, W., Ed.; Oxford University Press: Oxford, U.K., 1996; p 445. (b) Schurtenberger, P. *Light scattering in complex micellar systems in Light Scattering. Principles and Development*; Brown, W., Ed.; Oxford University Press: Oxford, U.K., 1996; p 296. (c) Higgins, J.; Benoit, H. C. *Polymers and Neutron Scattering*; Oxford University Press: Oxford, U.K., 1996; Chapter 7, p 241.
(62) Antonietti, M.; Heinz, S.; Schmidt, M.; Rosenauer, C. *Macromolecules* **1994**, *27*, 3276.
(63) Pitsikalis, M.; Siakali-Kioulafa, E.; Hadjichristidis, N. *Macromolecules* **2000**, *33*, 5460.

MA061396N